

# 원자현미경 리소그래피 : 양극전압 파형이 옥사이드 성장에 미치는 영향

## Atomic Force Microscope (AFM) Lithography : Influence of the Anodic Voltage Waveform on the Formation of Oxide Nanodots

#김철웅<sup>1</sup>, \*김태영<sup>2</sup>

<sup>#</sup>Cheol-Woong Kim ([woong25@korea.ac.kr](mailto:woong25@korea.ac.kr))<sup>1</sup> and <sup>\*</sup>Tae-Young Kim<sup>2</sup>

<sup>1</sup> 고려대학교/(주)트리플씨메디칼, <sup>2</sup>(주)트리플씨메디칼 R&D Center

Key words : Anodic Voltage Waveform, Atomic Force Microscope (AFM), Local Anodic Oxidation (LAO), Nanostructures

### 1. Introduction

Since the application of Atomic Force Microscope (AFM) local anodic oxidation in patterning nanometer-scale oxide features on silicon and metals, efforts have been made to control the oxide growth by tuning the operational parameters on nano-oxidation such as relative humidity, exposure time, amplitude of bias voltage and AFM operation mode<sup>1-3</sup>. This technique has enabled fabrication of a variety of prototype nanodevices<sup>4-7</sup>. All these works pointed out that the buildup of space charge causes self-limiting growth, therefore this effect should be minimized to obtain better performance of the oxidation process and higher aspect ratio (height/width) of oxide features<sup>8-12</sup>. In this paper we consider a conductive AFM tip-induced oxidation of a Ti film deposited on SiO<sub>2</sub>, under the application of different waveforms. We report on the main features of the fabricated TiO<sub>2</sub> nanodots, as it is known from the literature<sup>13</sup> that Ti is anodized to TiO<sub>2</sub>. We show how the use of different waveform voltages affects process control during oxide growth, providing higher flexibility in the oxide shaping.

### 2. Experimental Methods and Materials

All experiments of titanium oxide growth were carried out on samples prepared by evaporating a thin Ti film on a commercial p-type silicon wafer (1-10 ohm-cm) covered with 1,000Å of thermal SiO<sub>2</sub>. The measured thickness of the Ti layer was 7nm on average with a 0.5nm rms roughness and was obtained by using a quartz-crystal thickness and AFM imaging. All the AFM patterning and measurements were performed in contact mode at room temperature, 26-28 °C over the range of 40%-44% of relative humidity, using a commercial AFM system (PSIA, XE-100). Tips used in our experiments were silicon cantilevers coated with 20-30nm of TiN.

The height of the tip was in the range of 10-15nm with a typical curvature radius of 35nm. The sample was mounted onto the sample holder and a conductive bridge was formed between the Ti surface and the sample holder with Ag paste. The tip and sample holder set up were electrically isolated from the AFM unit. The AFM feedback circuit was always activated in order to maintain a constant tip-sample distance during imaging and patterning. A Keithley 236 source measure unit, capable of generating various voltage waveforms with the desired timing and shape, was integrated with the AFM system for tip biasing and simultaneous collection of current versus time (I-t) data. The I-t signals were transferred to and processed on a PC using the LABVIEW program. Two types of AFM oxidations were performed according to the chosen waveform voltage, a constant bias voltage and a linear ramp voltage, as shown in Fig. 1(a) and (b), respectively. Once specific positions were selected within the scan area, current data before pulling down the tip to the sample surface and after the tip approach were recorded in order to calculate the oxidation current by subtracting the detected current data before oxidation from those recorded during oxidation, as described in our previous work<sup>14</sup>.

### 3. Results and Discussion

Various symmetric ramp types of bias voltages were applied by varying the exposure time,  $T_d$ , from 50ms to 1,500ms and the peak voltage  $V_p$  from -10 to -15V. Fig. 1(a) shows two captured current waveforms during oxidation as a function of time and sweep voltage. These current waveforms obtained with different exposure times are similar in shape but exhibit different features. During the forward sweep, the onset of the oxidation current in nanoampere range takes place when the sweep voltage reaches a certain value which is defined as threshold voltage. This value is close to the one found in the constant bias voltage case for long  $T_d$ . At shorter  $T_d$ , which corresponds to faster voltage sweep, a higher threshold voltage is observed and a lower peak current is detected. The  $T_d$  dependency is also found on examining the temporal position of the peak current with respect to the voltage sweep. As  $T_d$  becomes shorter, the temporal position of the current peak shifts from forward to reverse sweep region. This means that, at shorter  $T_d$ , the current continues to increase for some time even in the reverse sweep where the voltage falls linearly. Evidence of this behaviour is given in Fig. 1(b), where a negative differential conductance  $dI/dV$  occurs for  $T_d = 400ms$ , while  $dI/dV$  is always constant for  $T_d = 1,500ms$ . Fig. 1(c) shows the height and volume growth with time of oxide dots as a function of  $T_d$ . It is found that the use of longer  $T_d$ , which corresponds to slower sweep rates, produced dots with increased height and larger lateral thickness, resulting in greater volume features. As a first approximation, a logarithmic law supports these data, as

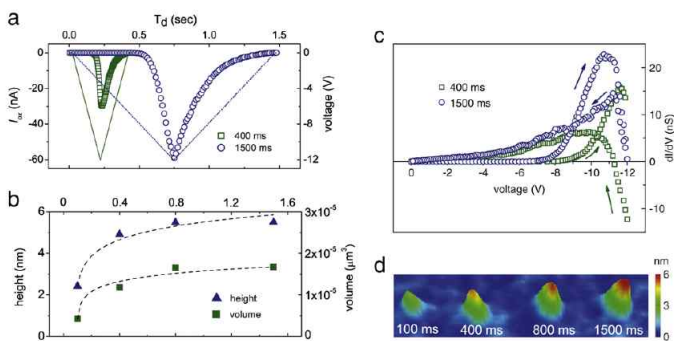


**Fig. 1** (a) Current versus time during oxidation performed under ramp voltage with  $V=-12V$  for two exposure times (400ms and 1500 ms),  $T_f = T_r = T_d/2$ ,  $R_f = R_r = V/T_f$ . Solid lines represent the corresponding bias voltage waveform. (b) Differential conductance  $dI/dV$  plot of (a), (c) Height and volume of the oxide dots obtained with different exposure times, (d) AFM images of (c).

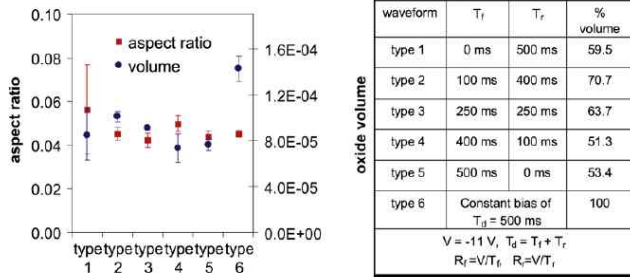


**Fig. 2** Performance estimation of various voltage waveforms on oxide growth (left), Aspect ratio and volume of oxide dots as a function of the applied waveforms whose parameters are reported in the table (right), Characteristic parameters of the waveforms used in this experiment and fractional percent of the volume of oxide dots fabricated by a ramp waveform (type 1- type 5) with respect to the one obtained at constant bias (type 6)

previously found for the constant bias voltage case. As expected, using longer  $T_d$  accounts for the increased growth of the fabricated nanodots (see Fig. 1(d)), which can also be related to the higher differential conductance with longer  $T_d$  exhibited in Fig. 1(b). Hence, the dependency of the threshold voltage on  $T_d$ , the temporal position of the current peak and the  $dI/dV$  behaviour are associated with the oxidation kinetics which led to the fabrication of the oxide dots. We estimated the waveform performance for growing oxide nanodots in terms of % volume and aspect ratio by changing the duty cycle defined as  $T_f/T_d$  ( $T_f$ : forward sweep duration). The % volume is defined as the fractional percent of the volume of oxide dots fabricated using a ramp waveform with respect to the one obtained at constant bias voltage with the same TI(time integration) and  $V_p$ . As shown in Fig. 2, the highest % volume (70.7%) was obtained using the asymmetrical type 2 waveform, while the symmetric waveform, type 3, produced 63.7% of volume. The aspect ratio obtained using the type 4 waveform was higher than the one of type 6 (constant bias) and of type 3 (symmetric linear ramp) by 10% and 20%, respectively. Type 1 and type 5 waveforms are extreme cases with duty cycles equal to 0 and 1, respectively. In this way, the change of duty cycle which leads to the complementary change of  $R_f$  ( $R_f$ : forward sweep rate) and  $R_r$  ( $R_r$ : reverse sweep rate) with the same TI results in a "tuning" effect for the control of oxide volume and aspect ratio. A bias voltage with a higher duty cycle can be tuned to fabricate higher aspect ratio oxides, while a lower duty cycle results in features with higher volume. Nevertheless, it should be considered that the aspect ratio enhancement obtained with the type 1 waveform appears overestimated owing to the high standard deviation. Finally, it is worth mentioning that the use of a voltage modulation technique with pulsed asymmetrical waveforms might turn out to be a flexible nanolithographic strategy. If a high duty cycle waveform were to be used in a pulsed way, it may be expected to obtain oxide dots with higher volume. If instead, waveforms of low duty cycle were used, fabrication of oxide dots with high aspect ratio is expected.

**4. Conclusions**

We investigated the influence of voltage waveform in AFM anodic oxidation on titanium by analyzing the current behaviour and the morphology of fabricated oxide nanodot features. The application of the ramp bias voltage allows higher control of oxide nanodot

features in terms of volume and height. Under the same time integration parameter TI, ramp waveforms with high duty cycles produce more voluminous oxide dots while ramp waveforms with low duty cycles produce oxide dots with enhanced aspect ratio.

**References**

1. P. Avouris, T. Hertel, R. Martel, "Atomic Force Microscope Tip Induced Local Oxidation of Silicon: Kinetics, Mechanism, and Nanofabrication," *Appl. Phys. Lett.*, 71, 285, 1997.
2. H. Kuramochi, K. Ando, H. Yokoyama, "Effect of Humidity on Nano-oxidation of p-Si(0 0 1) Surface," *Surf. Sci.* 542, 56, 2003.
3. N. Clement, D. Tonneau, B. Gely, H. Dallaporta, V. Safarov, J. Gautier, "High Aspect Ratio Nano-oxidation of Silicon with Noncontact Atomic Force Microscopy," *J. Vac. Sci. Technol. B*, 21, 2348, 2003.
4. P. M. Campbell, E. S. Snow, P. J. McMarr, "Fabrication of Nanometer-scale Side-gated Silicon Field Effect Transistors with an Atomic Force Microscope," *Appl. Phys. Lett.*, 66,1388,1995.
5. U. F. Keyser, H. W. Schumacher, U. Zeitler, R. J. Haug, "Fabrication of a Single-electron Transistor by Current-controlled Local Oxidation of a Two-dimensional Electron System," *Appl. Phys. Lett.*, 76, 457, 2000.
6. K. Matsumoto, Y. Gotoh, T. Maeda, "Room-temperature Single-electron Memory made by Pulse-mode Atomic Force Microscopy Nano Oxidation Process on Atomically Flat  $\alpha$ -alumina Substrate," *Appl. Phys. Lett.*, 76, 239, 2000.
7. F. H. Chiu, F. C. Chiu, S. K. Fan, K. C. Tai, J. Y. Lee, "Electrical Characterization of Tunnel Insulator in Metal/insulator Tunnel Transistors Fabricated by Atomic Force Microscope," *Appl. Phys. Lett.*, 87, 243, 506, 2005.
8. J. A. Dagata, J. Itoh, K. Matsumoto, H. Yokoyama, "Role of Space Charge in Scanned Probe Oxidation," *J. Appl. Phys.*, 84, 6891, 1998.
9. E. Dubois, J. L. Bubendorff, "Kinetics of Scanned Probe Oxidation: Space-charge Limited Growth," *J. Appl. Phys.*, 87, 8148, 2000.
10. J. A. Dagata, F. Perez-Murano, G. Abadal, K. Morimoto, T. Inoue, J. Itoh, H. Yokoyama, "Predictive Model for Scanned Probe Oxidation Kinetics," *Appl. Phys. Lett.*, 76, 2710, 2000.
11. J. A. Dagata, *et al.*, "Current, Charge, and Capacitance during Scanning Probe Oxidation of Silicon (I) Maximum Charge Density and Lateral Diffusion," *J. Appl. Phys.*, 96, 2386, 2004.
12. J. A. Dagata, *et al.*, "Current, Charge, and Capacitance during Scanning Probe Oxidation of Silicon (II) Electrostatic and Meniscus Forces Acting on Cantilever Bending," *J. Appl. Phys.*, 96, 2393, 2004.
13. H. Sugimura, T. Uchida, N. Kitamura, H. Masuhara, "Scanning Tunneling Microscope Tip-induced Anodization of Titanium: Characterization of the Modified Surface and Application to the Metal Resist Process for Nanolithography," *J. Vac. Sci. Technol. B*, 12, 2884, 1994.
14. T.Y. Kim, D. Ricci, E. Di Zitti, S. Cincotti, "A Study of the Transient Current during the Formation of Titanium Oxide Nanodots by AFM Anodic Oxidation," *Surf. Sci.*, 601, 4910, 2007.